Electronic Supplementary Material (ESI) for ChemComm.

Supporting Information

Electrochemical Behaviour of Uranium at a Tripolyphosphate Modified ITO Electrode

Xiangyang Hou,[a] Jeffrey R. McLachlan,[a] Christopher J. Dares [a],*

[a] Department of Chemistry and Biochemistry, Florida International University, Miami, FL 33199, USA

email: cdares@fiu.edu

Experimental Section

With the exception of uranyl acetate and uranyl nitrate, which were donated by FIU Environmental Health and Safety through an existing stockpile, all chemicals and solvents were purchased through Fisher Scientific and used as received without further purification, unless otherwise stated. Fluorine-doped tin oxide (FTO) sputtered coated glass was purchased from Hartford Glass, Inc. All other non-fabricated electrodes were purchased from CH Instruments. Electrochemical experiments were performed using a CH Instruments 630E potentiostat. CV and SWV experiments were performed using a single compartment cell, an SCE reference electrode, and a carbon-rod counter electrode. Bulk electrolysis to prepare U^{4+} was performed in a 2-compartment cell using a Pt coil electrode for bulk reduction at -0.45 V and characterized by UV-vis spectroscopy. Spectroelectrochemical reduction of UO_2^{2+} was performed in a 2-compartment cell comprised of square pyrex glass with a path length of 1.00 cm. The *n*ITO electrodes in these experiments was oriented so the light passed through the *n*ITO electrode parallel to the normal of the *n*ITO surface. A blank spectrum was acquired after applying -0.40 V for 1 min to the working electrode in a solution without uranium. XPS spectra were collected on a Kratos Axis Ultra DLD X-ray photoelectron spectrometer with a monochromatic Al K_α source for high resolution work. Energy correction was achieved setting the lowest energy binding component of the C 1s peak to 284.6 eV.

*n*ITO electrodes were fabricated according to published procedures.[1] Briefly, ITO ethanol dispersion (In_2O_3:SnO_2 = 95:5, 18 nm, 20 wt %, Blue) was diluted to 15 wt % with 200 proof ethanol. The 15 wt% dispersion was sonicated for an hour in a sonicating bath to ensure homogeneity. Under vigorous stirring, 0.433 g of hydroxypropyl cellulose (HPC) was slowly added to 20 mL of the 15 wt % ITO ethanol dispersion to yield a 15 wt% ITO, 2.5 wt% HPC suspension. The resulting suspension was ultrasonicated using a sonicating horn for 10 minutes (3 s on, 3 s off interval). The suspension was sonicated in a sonicating bath overnight and was ready for use the next morning. A sheet of FTO was cleaned with ethanol and allowed to dry in the air. Two layers of scotch tape were placed on the FTO sheet about 1 cm apart. A drop about 1 cm in diameter was applied 1 cm from the edge of the FTO sheet between the two pieces of tape.

The long side of a glass pipette was used to spread the suspension along the entire channel formed from the tape strips. While the suspension was wet, the tape was removed. A Thermo Scientific Lindberg Blue M Programable Oven was used to anneal the electrodes at 500 °C for 3 hours. Once annealed, the electrodes were ready for use.

*n*ITO|P_3 electrodes were prepared by soaking a *n*ITO electrode in a 2 mM solution of sodium tripolyphosphate in 0.1 M $HClO_4$ for 24 h. Electrodes were rinsed 3-times with fresh 0.1 M $HClO_4$ before use. Given the redox inactivity of the P_3 ligand, and their lack of spectroscopic signals, surface coverage was determined after soaking the electrode in a 1 mM solution of UO_2^{2+} in 0.1 M $HClO_4$. The surface coverage was determined by dividing the cumulative charge passed during UO_2^{2+} reduction by the Faraday constant, electrode area, and number of electrons transferred (2). A maximum surface coverage of 8.5 nmol/cm^2 was obtained and is consistent with expectations for a well-packed monolayer of P_3 at *n*ITO with one uranium moiety per ligand.

CVs used for foot-of-the-wave (FOTW) analysis were acquired at 50mV/s. The UO_2^{2+} reduction potential was measured using CV experiments as the potential where the peak current is observed. These values are reported in Table S2. The FOTW analysis plot was prepared by plotting Equation 11 based on work by Savéant and co-workers.[2] In the linear region of the plot side phenomena including the consumption of substrate (UO_2^{2+}), deactivation of the catalyst via inhibition by the product (generated by U^{4+} occupation of binding sites) are significant. The influence of these processes are insignificant at the onset of catalysis (beginning of the reduction of UO_2^{2+}, or foot of the wave). The slope in the initial rising region was therefore used to determine k_{obs}.

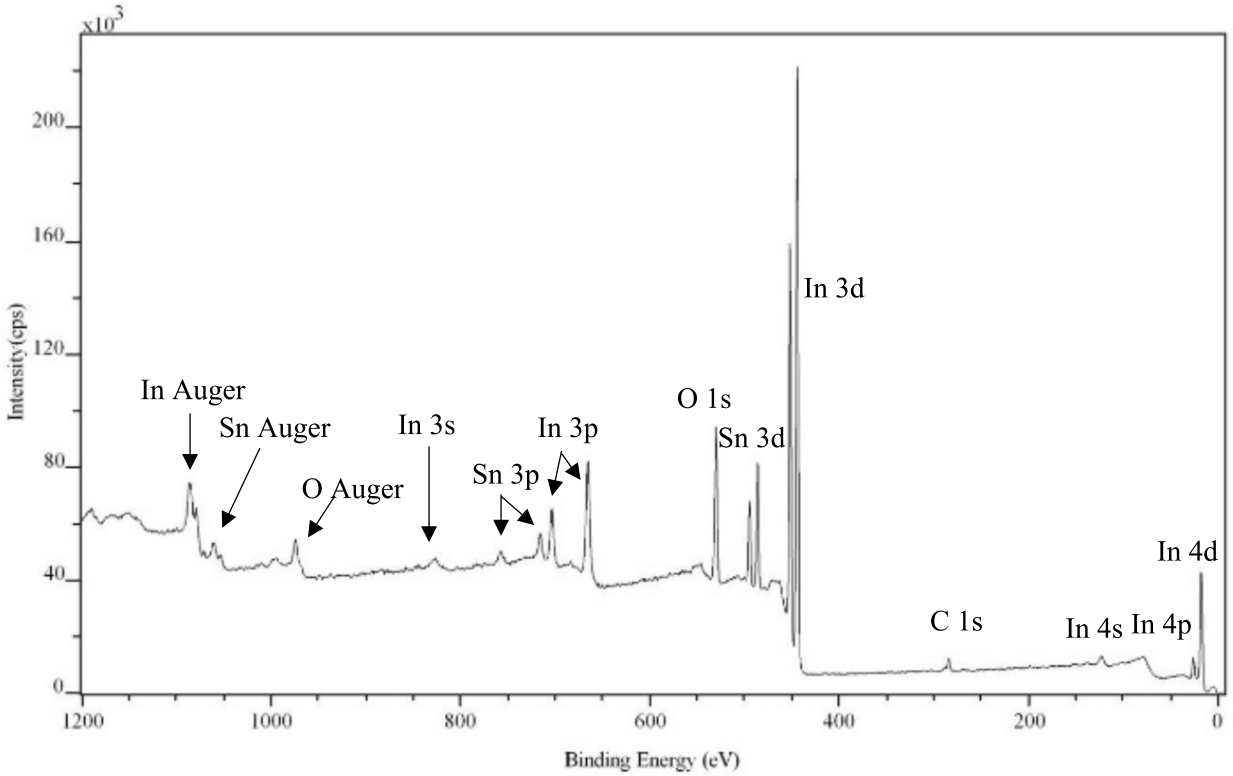

Figure S1. Survey XPS scan of a bare *n*ITO electrode.

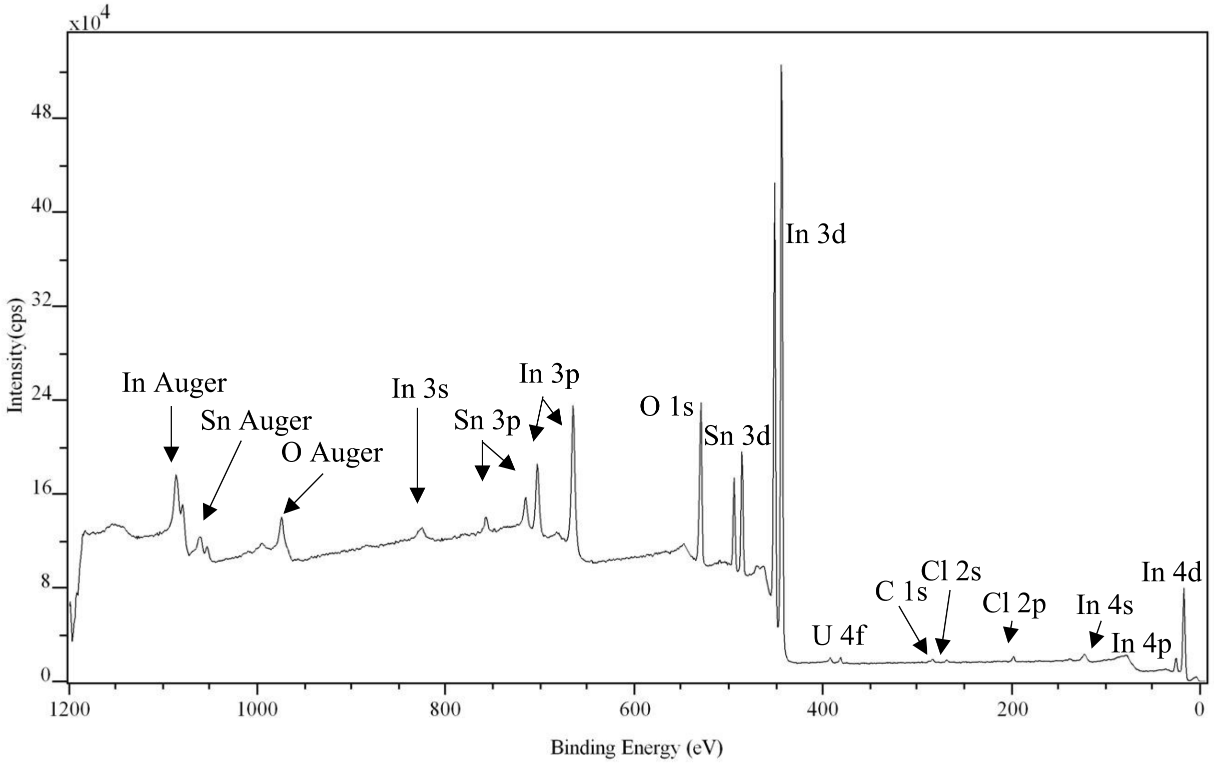

Figure S2. Survey XPS scan of a bare *n*ITO electrode after 30 min bulk reduction at -0.4 V of a 10 mM solution of UO_2^{2+} in 0.1 M $HClO_4$.

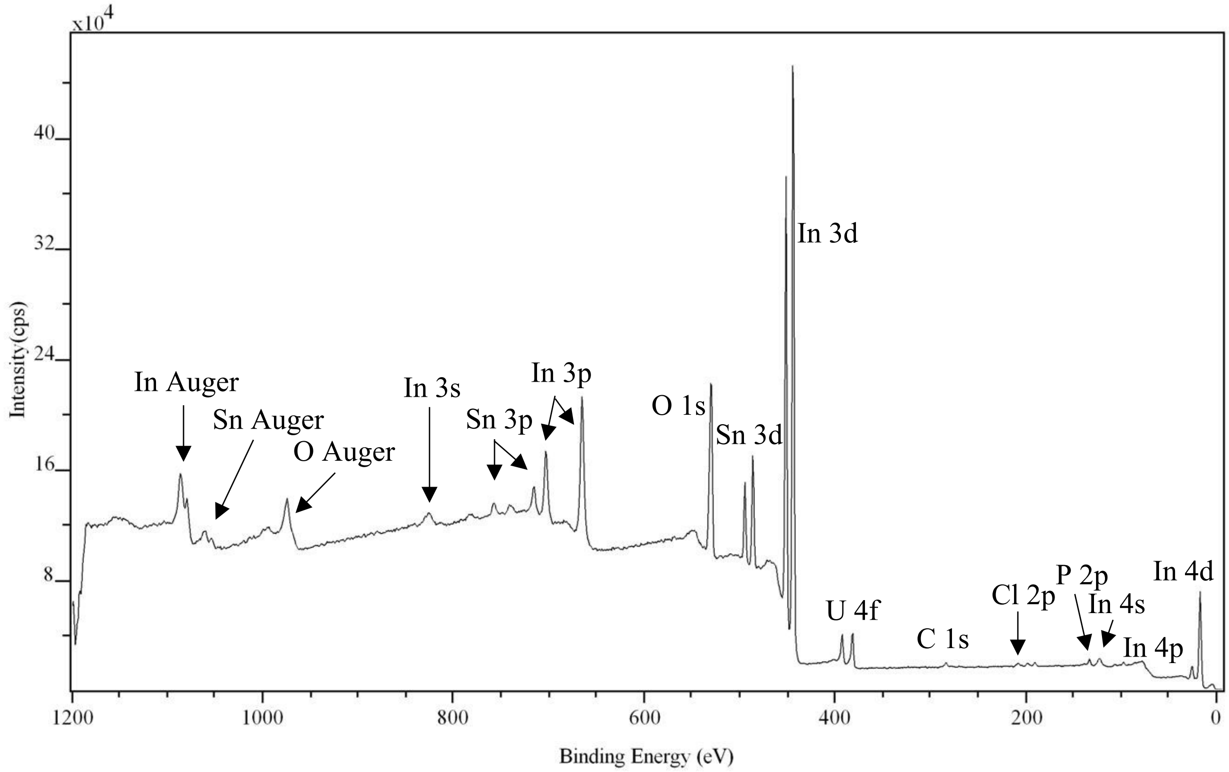

Figure S3. Survey XPS scan of *n*ITO|P_3 electrode soaked in a 0.1 M $HClO_4$ solution with 10 mM UO_2^{2+}.

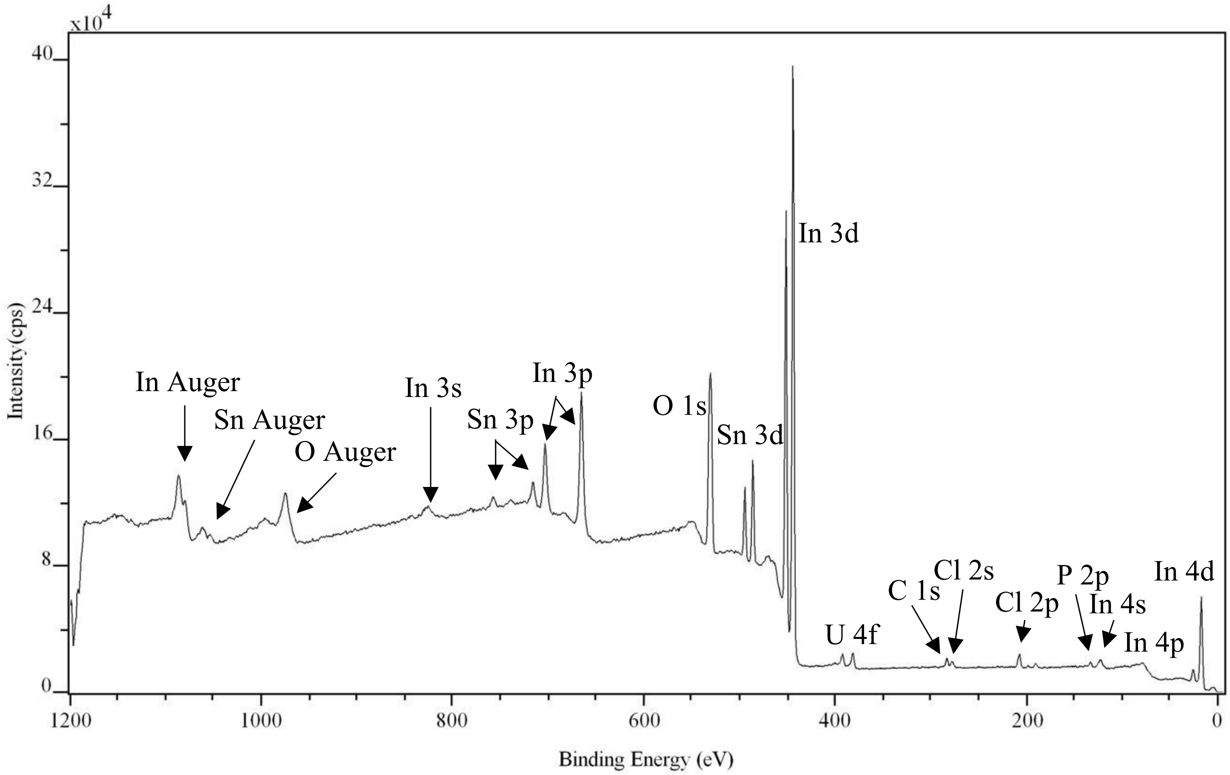

Figure S4. Survey XPS scan of *n*ITO|P_3 electrode soaked in a 0.1 M $HClO_4$ solution with 10 mM U^{4+}.

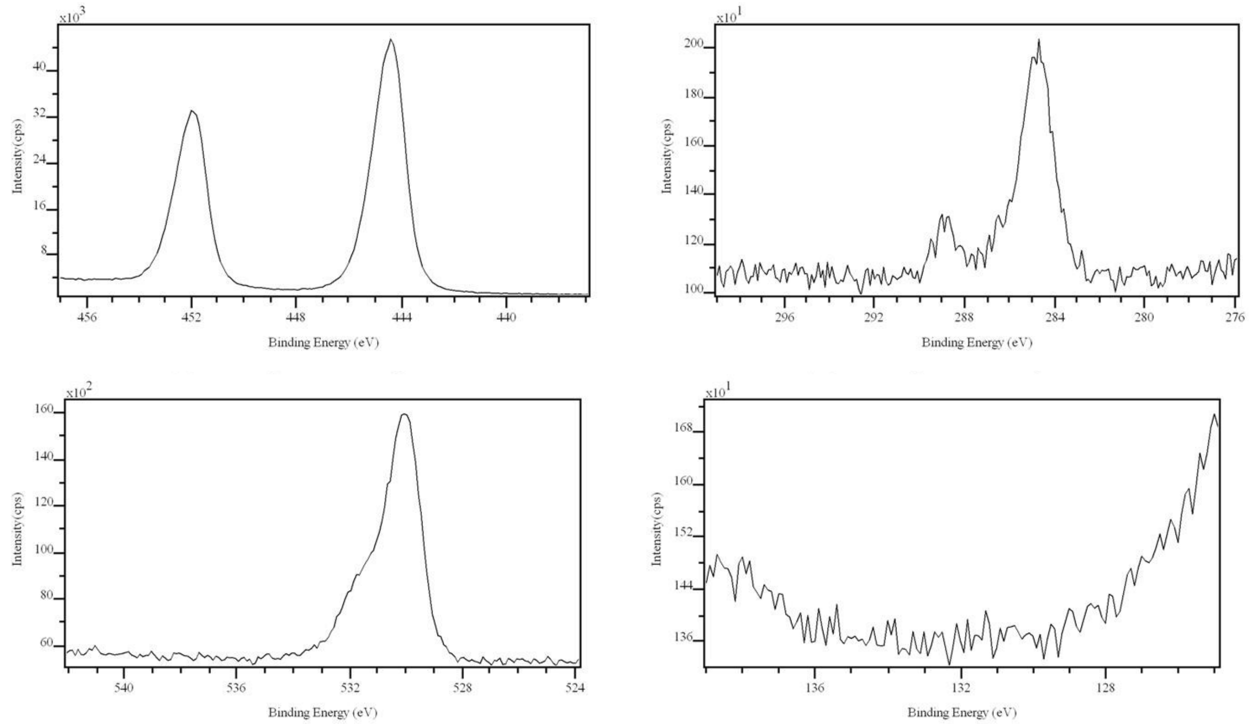

Figure S5. High resolution XPS scans of a bare *n*ITO electrode featuring the In 3d signals (**top left),** the C1s signals (**top right**), the O1s signal (**bottom left**), and the lack of any P 2p signals (**bottom right**).

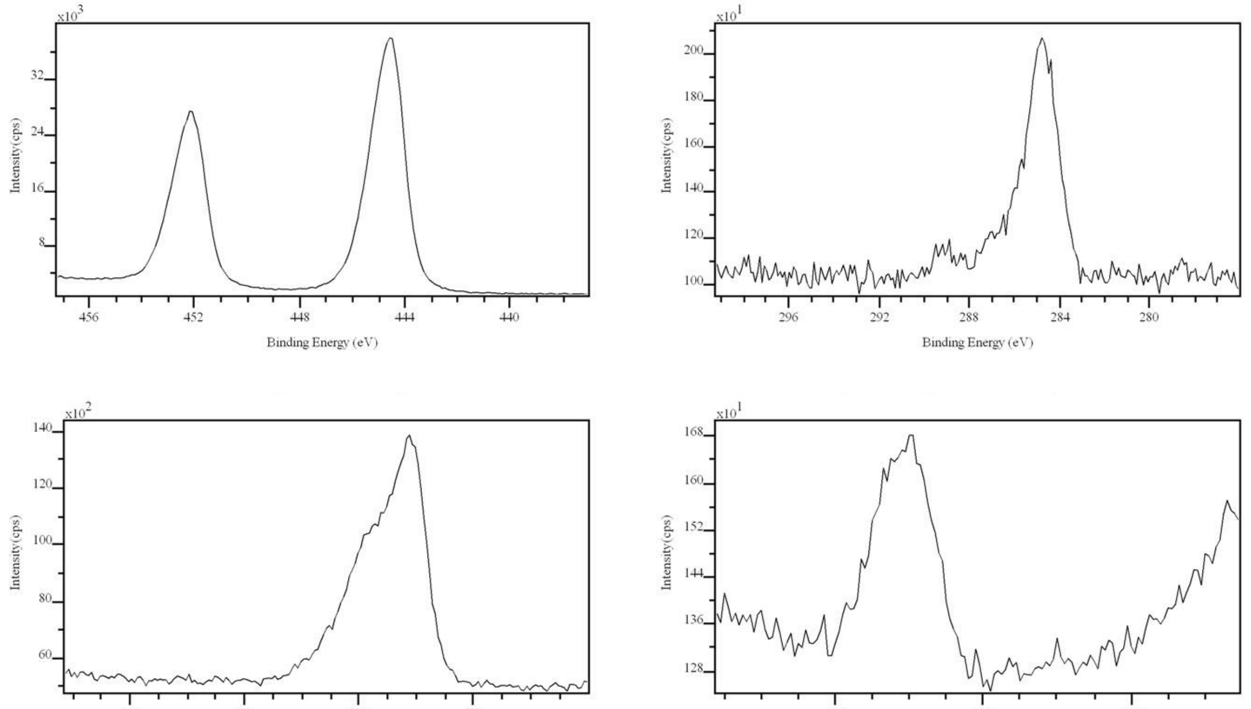

Figure S6. High resolution XPS scans of a *n*ITO|P_3 electrode featuring the In 3d signals (**top left),** the C1s signals (**top right**), the O1s signal (**bottom left**), and the P 2p signals (**bottom right**).

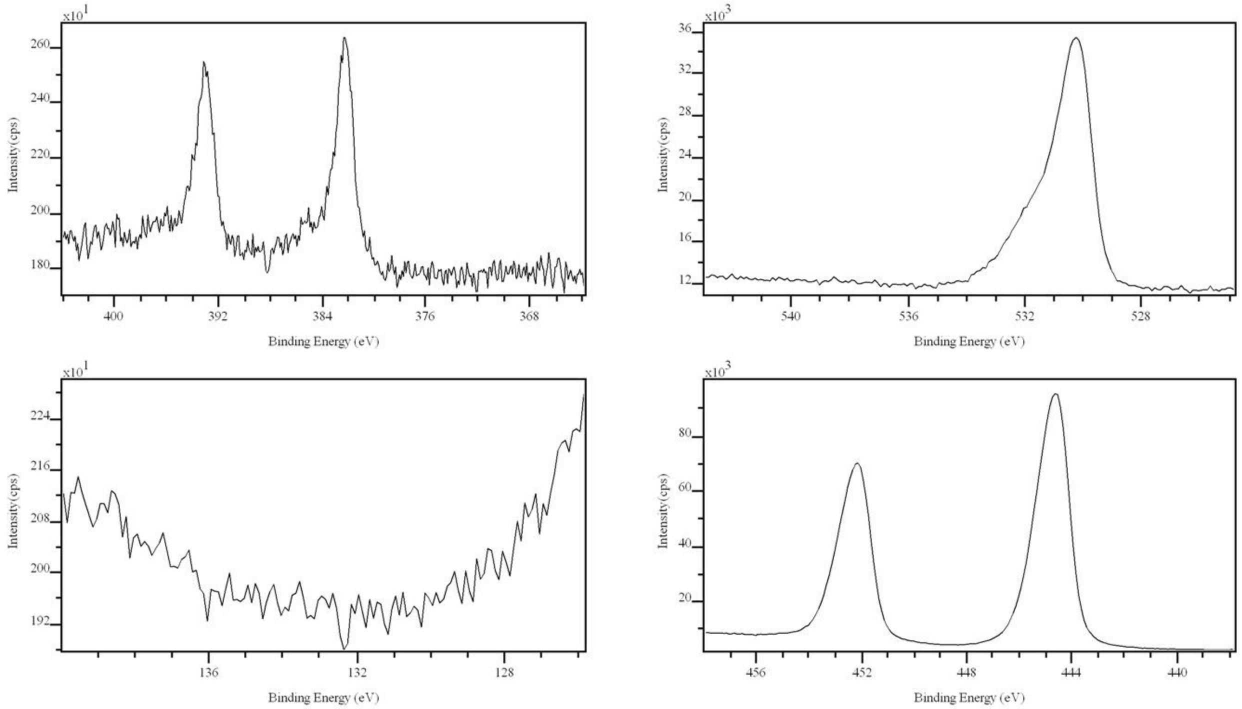

Figure S7. High resolution XPS scans of a bare *n*ITO electrode after 30 min bulk reduction at -0.4 V of a 10 mM solution of UO_2^{2+} in 0.1 M $HClO_4$ featuring the U 4f signals (**top left),** the O 1s signals (**top right**), the P 2p signal (**bottom left**), and the In 3d signals (**bottom right**).

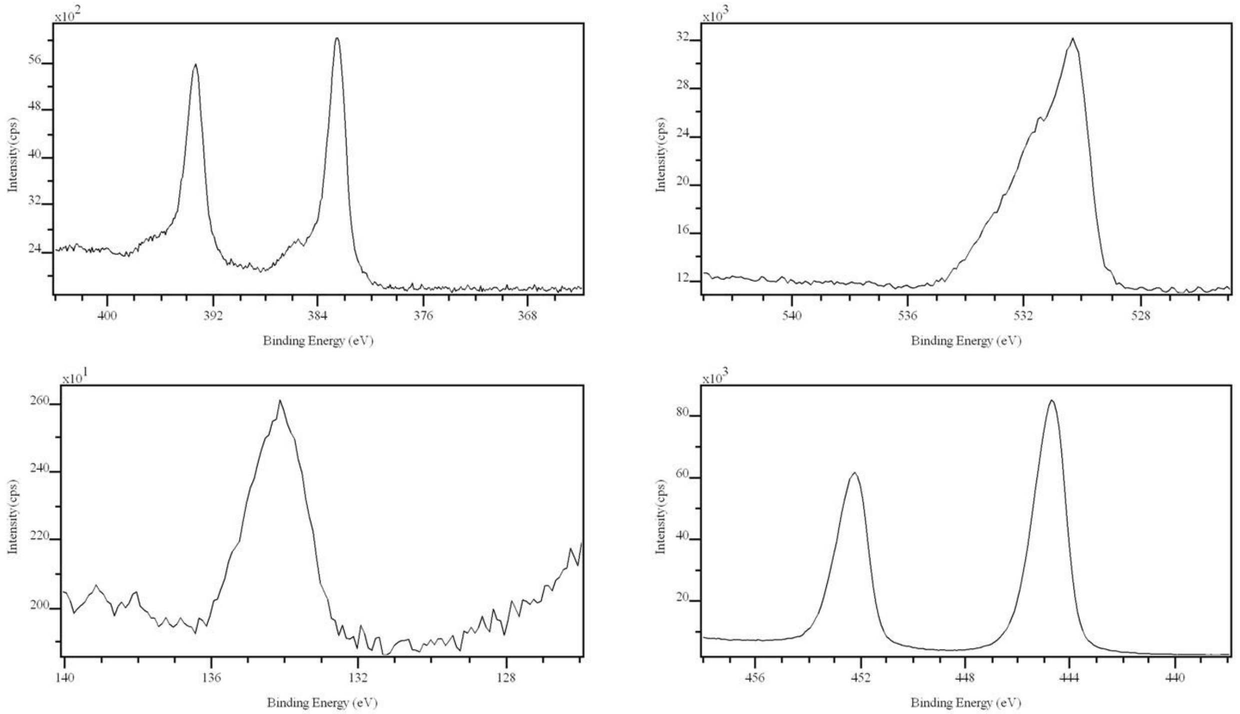

Figure S8. High resolution XPS scans of a *n*ITO|P_3 electrode soaked in 0.1 M $HClO_4$ with 10 mM UO_2^{2+} featuring the U 4f signals (**top left),** the O 1s signals (**top right**), the P 2p signal (**bottom left**), and the In 3d signals (**bottom right**).

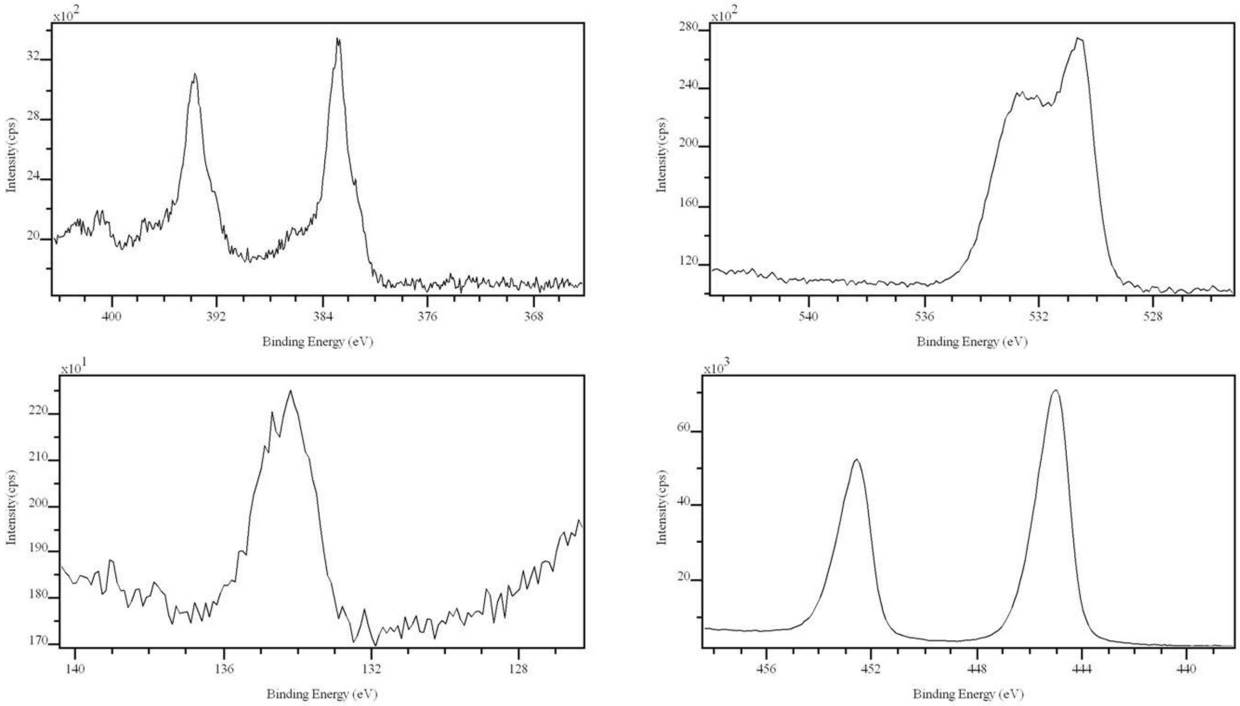

Figure S9. High resolution XPS scans of a *n*ITO|P_3 electrode soaked in 0.1 M $HClO_4$ with 10 mM U^{4+} featuring the U 4f signals (**top left),** the O 1s signals (**top right**), the P 2p signal (**bottom left**), and the In 3d signals (**bottom right**).

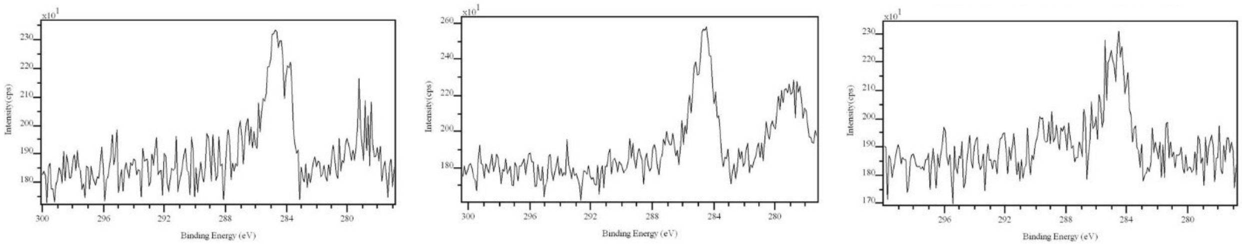

Figure S10. High resolution XPS spectra of the C 1s signals for a *n*ITO|P_3 electrode soaked in 0.1 M $HClO_4$ with 10 mM UO_2^{2+} (Left); a *n*ITO|P_3 electrode soaked in 0.1 M $HClO_4$ with 10 mM U^{4+} (Middle); a bare *n*ITO electrode after 30 min of electrolysis at -0.4 V in 0.1 M $HClO_4$ with 10 mM UO_2^{2+} (Right).

Table S1. Summary of XPS signals for bare *n*ITO from high resolution scans.

Element (signal)	Energy (eV)	FWHM (eV)	Atomic Conc. (%)	Mass Conc. (%)
In(3d)	444.30	1.43	31.7	78.0
O(1s)	529.95	1.60	52.0	17.8
C(1s)	284.60	1.60	16.3	4.2

Table S2. Summary of XPS signals for *n*ITO|P_3 from high resolution scans.

Element (signal)	Energy (eV)	FWHM (eV)	Atomic Conc. (%)	Mass Conc. (%)
In(3d)	444.40	1.49	27.3	73.3
O(1s)	530.05	2.48	53.2	19.9
C(1s)	284.60	1.56	16.5	4.6
P(2p)	133.70	1.89	3.1	2.2

Table S3. Summary of XPS signals for a bare *n*ITO electrode after 30 min of electrolysis at -0.40 V in 0.1 M $HClO_4$ with 10 mM UO_2^{2+} from high resolution scans.

Element (signal)	Energy (eV)	FWHM (eV)	Atomic Conc. (%)	Mass Conc. (%)
In(3d)	444.70	1.46	35.6	79.4
O(1s)	530.30	1.59	60.7	18.9
C(1s)	284.60	1.45	3.6	0.8
U(4f)	382.35	1.49	0.2	0.9

Table S4. Summary of XPS signals for *n*ITO|P_3 soaked in 0.1 M $HClO_4$ with 10 mM UO_2^{2+} from high resolution scans.

Element (signal)	Energy (eV)	FWHM (eV)	Atomic Conc. (%)	Mass Conc. (%)
In(3d)	444.60	1.42	28.5	70.6
O(1s)	530.20	2.46	64.1	22.1
C(1s)	284.60	1.80	3.7	1.0
P(2p)	134.00	1.80	2.8	1.8
U(4f)	382.45	1.62	0.9	4.4

Table S5. Summary of XPS signals for *n*ITO|P_3 soaked in 0.1 M $HClO_4$ with 10 mM U^{4+} from high resolution scans.

Element (signal)	Energy (eV)	FWHM (eV)	Atomic Conc. (%)	Mass Conc. (%)
In(3d)	445.10	1.48	25.5	69.5
O(1s)	530.80	3.50	66.4	25.2
C(1s)	284.60	1.39	5.8	1.7
P(2p)	134.30	1.77	1.9	1.4
U(4f)	383.05	1.80	0.4	2.3

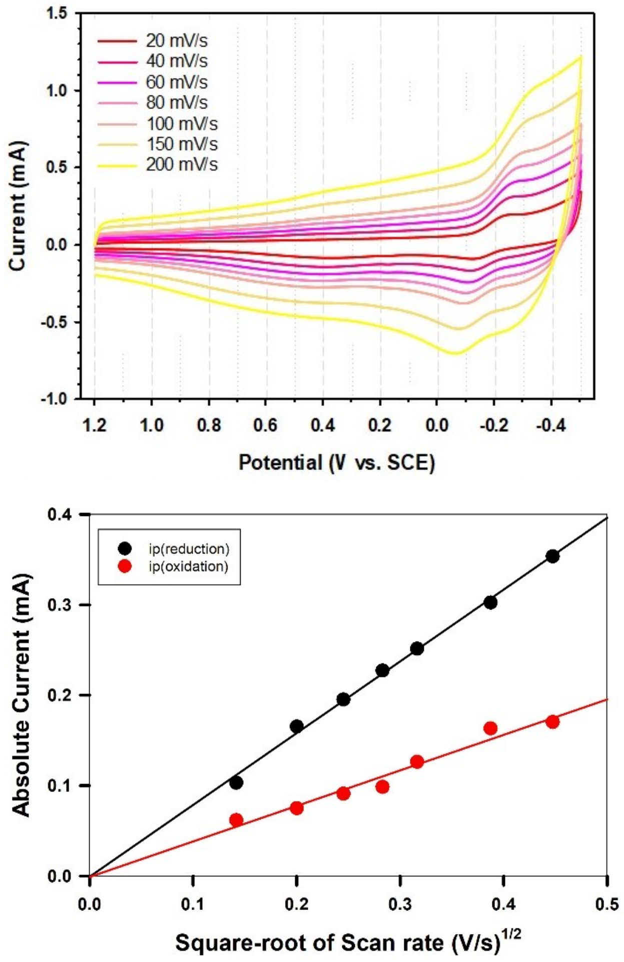

Figure S11. (Left) CVs of 1 mM UO_2^{2+} at bare nITO electrode in 0.1 M $HClO_4$ at various scan rates. (Right) Plot of peak currents for the cathodic event at -0.25 V and the anodic event at -0.1 V vs. the square root of scan rate.

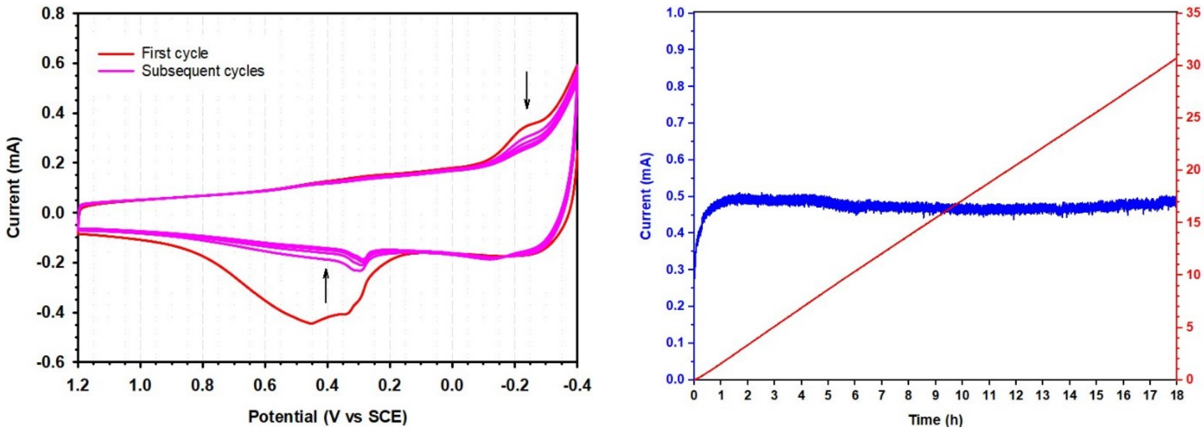

Figure S12. CVs of a bare nITO electrode in fresh 0.1 M $HClO_4$ (left) at 50 mV/s after bulk electrolysis (right) in 1 mM UO_2^{2+} in 0.1 M $HClO_4$ at -0.4 V for 18 h.

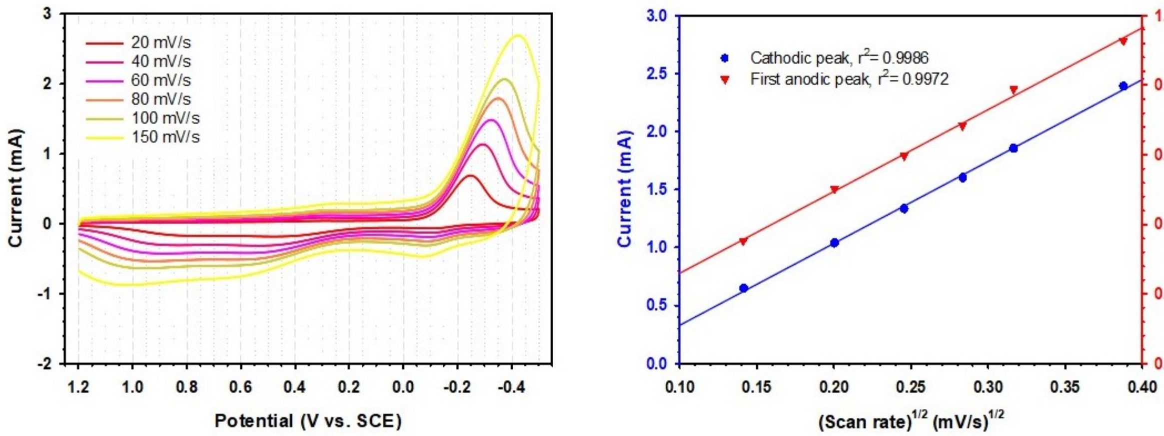

Figure S13. (Left) CVs of 1 mM UO_2^{2+} in 0.1 M $HClO_4$ at nITO|P_3 electrode at various scan rates. (Right) Plot of cathodic peak current and first anodic peak current versus square root of scan rate.

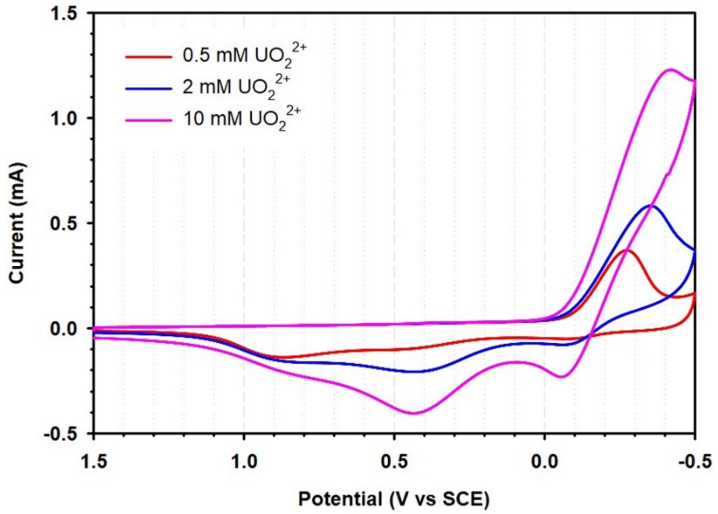

Figure S14. CVs of nITO|P_3 electrode in multiple UO_2^{2+} concentrations in 0.1 M $HClO_4$ at a scan rate of 20 mV/s.

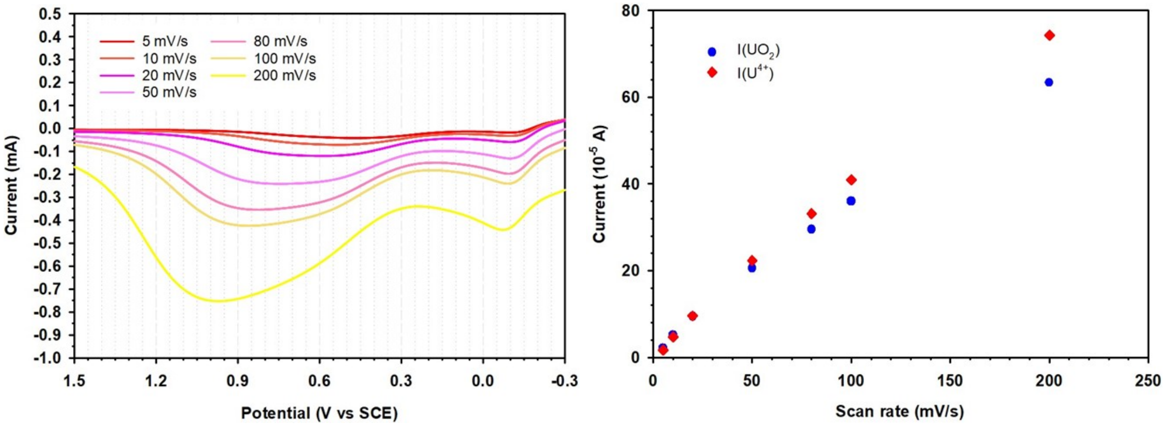

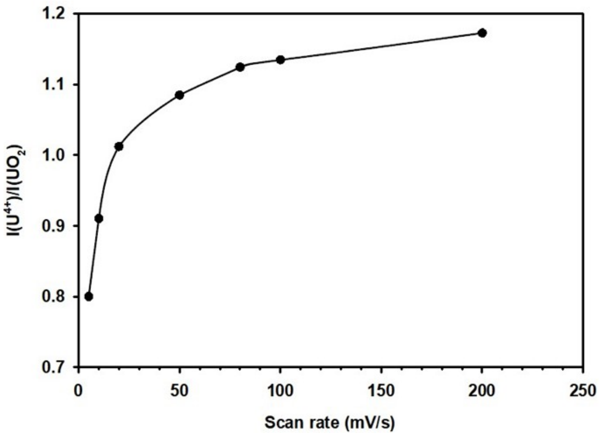

Figure S15. Top left: LSVs at nITO|P_3 electrode in 0.1 M $HClO_4$ with 1 mM UO_2^{2+} from -0.3 V to 1.5 V at various scan rates; Top right: peak current of the UO_2 and U^{4+} oxidations at a nITO|P_3 electrode using the LSVs in the Top left. Bottom: Relationship between the peak current ratio between the U^{4+} and UO_2 oxidations from the LSVs and the scan rate.

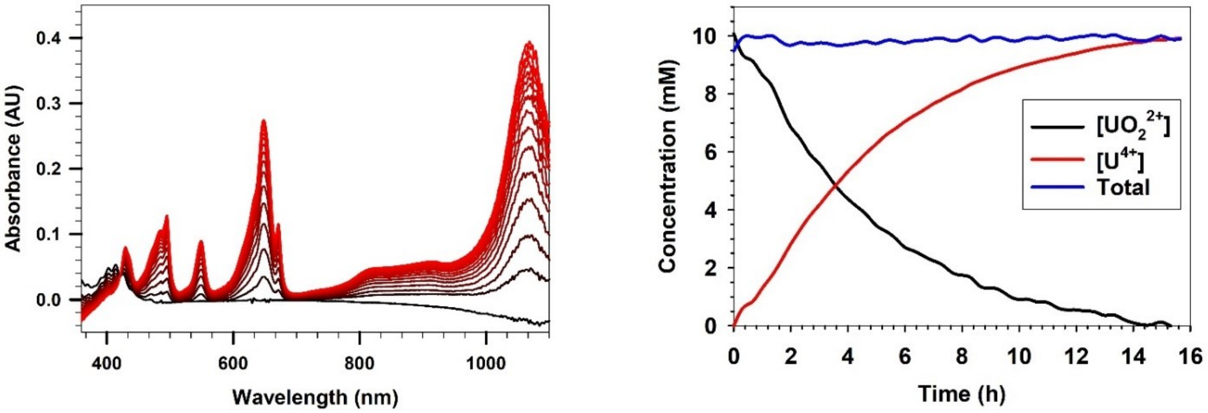

Figure S16. The UV-vis spectra (left) during the bulk electrolysis at -0.40 V of a 10 mM solution of UO_2^{2+} in 0.1 M $HClO_4$ with a total volume of 2.0 mL using a bare *n*ITO electrode. (Right) uranium speciation with time during electrolysis. The working electrode was placed perpendicular to the light path of the spectrometer resulting in minor spectroscopic signals from the electrode. A total of 5.7 C of charge was passed in the 15h 40 min duration of the bulk electrolysis equating to a Faradaic efficiency of 68 %. The first order rate constant associated with the appearance of U^{4+} is 2.8×10^{-3} min^{-1}.

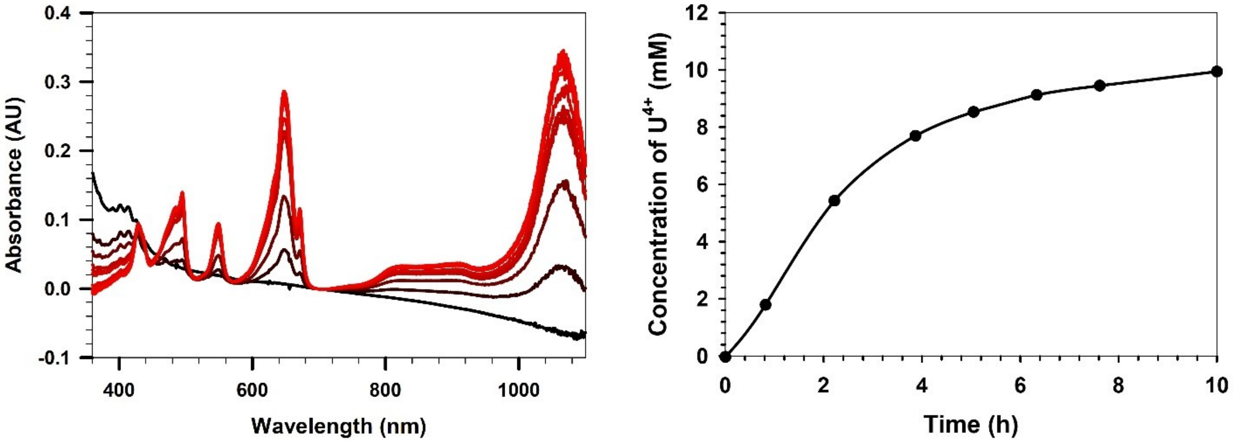

Figure S17. The UV-vis spectra (left) during the bulk electrolysis at -0.40 V of a 10 mM solution of UO_2^{2+} in 0.1 M $HClO_4$ with a total volume of 2.0 mL using a *n*ITO|P_3 electrode. (Right) uranium speciation with time during electrolysis. The working electrode was placed perpendicular to the light path of the spectrometer resulting in minor spectroscopic signals from the electrode. A total of 4.4 C of charge was passed in the 10 h duration of the bulk electrolysis equating to a Faradaic efficiency of 88 %. The first order rate constant associated with the appearance of U^{4+} is 5.4×10^{-3} min^{-1}.

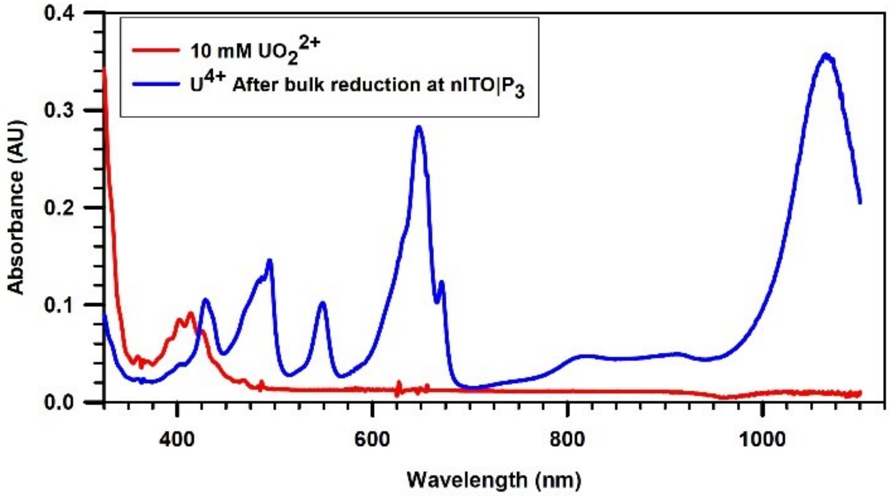

Figure S18. The initial (red) and final (blue) UV-vis spectra in a cuvette associated with bulk reduction from Figure S17.

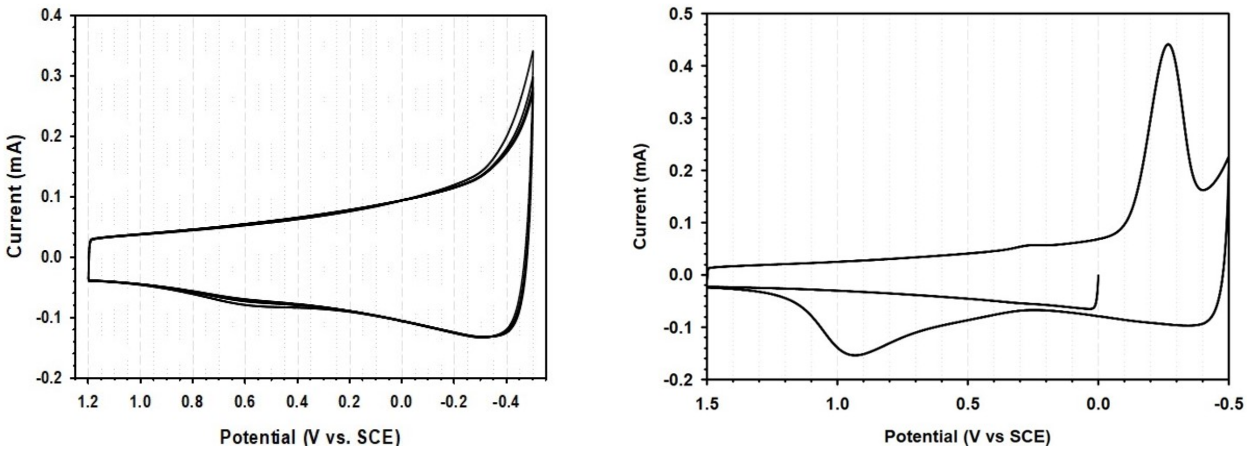

Figure S19. CVs of bare nITO (Left) and nITO|P_3 (Right) in fresh 0.1 M $HClO_4$ at a scan rate of 50 mV/s after soaking in 1 mM UO_2^{2+} in 0.1 M $HClO_4$ for 10 min. Electrodes were rinsed 3-times with 0.1 M $HClO_4$ before data collection. CVs with bare nITO start and end at 1.2 V, while CVs with nITO|P3 start at 0 V and scan first to +1.5 V then to -0.5 V, ending at +1.5V. Surface coverage of uranium at *n*ITO|P_3 is calculated to be 8.5 nmol/cm^2 based on the charge passed during the reduction at -0.25 V.

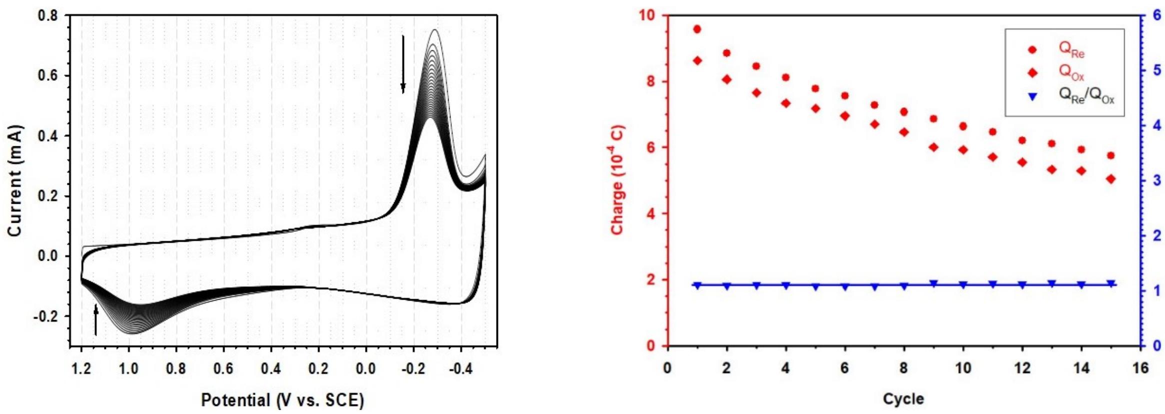

Figure S20. CV cycles of nITO|P_3 (Top) in fresh 0.1 M $HClO_4$ at a scan rate of 50 mV/s after soaking in 1 mM UO_2^{2+} in 0.1 M $HClO_4$ for 10 min; and the corresponding loss of adsorbed uranium based on the reduction at -0.25 V and oxidation at 1.0 V. The initial surface coverage is 8.5 nmol/cm^2. The electrode area was 1.00 cm^2.

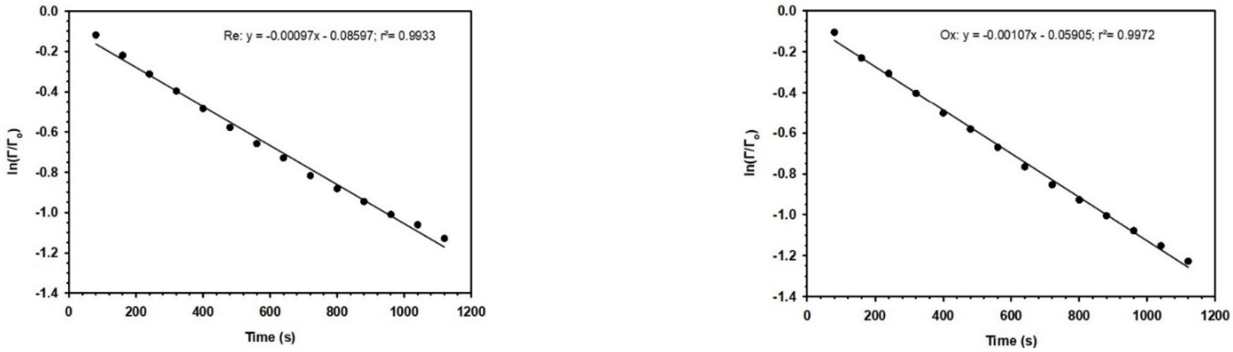

Figure S21. Dissociation of UO_2^{2+} (left) and U^{4+} (right) determined from the sequential CV cycles in Figure S20 for *n*ITO|P_3 electrodes soaked in 1 mM U^{4+} and rinsed before subsequent use in a fresh solution of 0.1

M $HClO_4$. The first order rate constant for the dissociation of UO_2^{2+} from *n*ITO|P_3 is 9.7×10^{-4} s^{-1} and is 11×10^{-4} s^{-1} for the dissociation of U^{4+}.

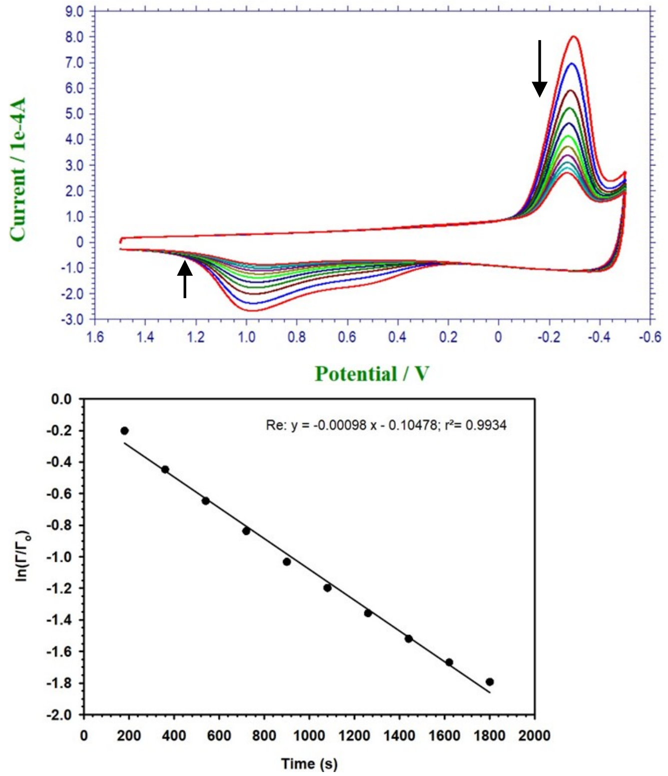

Figure S22. CV cycles of nITO|P_3 (Top) in fresh 0.1 M $HClO_4$ after soaking in 1 mM UO_2^{2+} in 0.1 M $HClO_4$ for 10 min (Left). CVs were acquired at a scan rate of 50 mV/s with a 3 minute interval between cycles. The first order rate constant associated with UO_2^{2+} dissociation with time (Left) based on the reduction at -0.25 V was determined to be 9.8×10^{-4} s^{-1}.

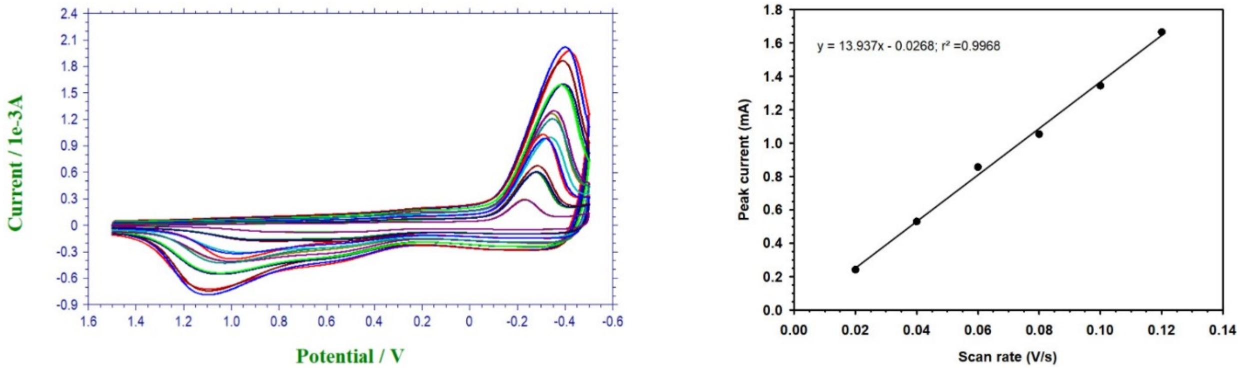

Figure S23. CVs (Left) at scan rates ranging from 20 mV/s to 120 mV/s of *n*ITO|P_3 in fresh 0.1 M $HClO_4$ after being soaked in 2 mM UO_2^{2+} for three minutes and then rinsed three times with 0.1 M $HClO_4$. Re-soaking the electrode in the uranyl solution between scans ensures complete adsorption of uranyl for each scan. CVs at each scan rate were acquired in triplicate to account for slight variations in the concentration of adsorbed uranyl. The peak current associated with the reduction of UO_2^{2+} at -0.25 V is linear with respect to the scan rate (Right) indicating a surface-bound redox event.

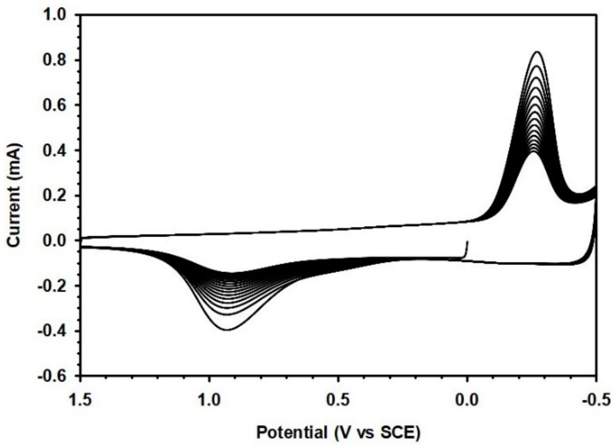
Current (mA)
1.0
0.8
0.6
0.4
0.2
0.0
-0.2
-0.4
-0.6
1.5
1.0
0.5
0.0
-0.5
Potential (V vs SCE)

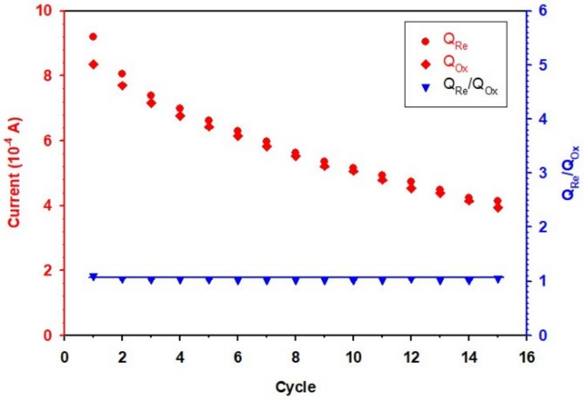
Q_{Re}
Q_{Ox}
Q_{Re}/Q_{Ox}
Current (10^{-4} A)
Q_{Re}/Q_{Ox}
10
8
6
4
2
0
6
5
4
3
2
1
0
0
2
4
6
8
10
12
14
16
Cycle

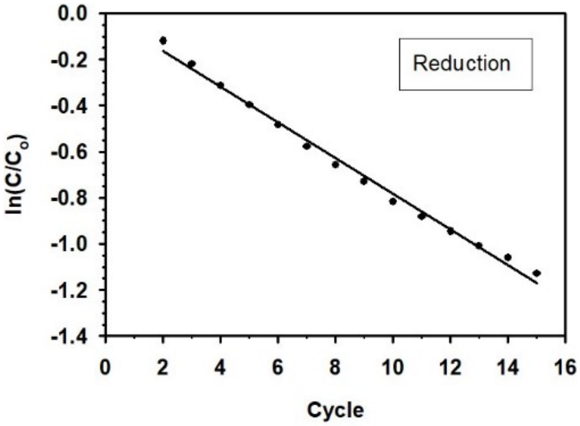
Reduction
ln(C/C$_o$)
0.0
-0.2
-0.4
-0.6
-0.8
-1.0
-1.2
-1.4
0
2
4
6
8
10
12
14
16
Cycle

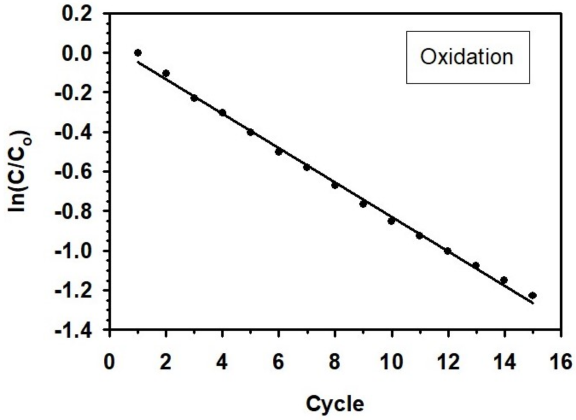
Oxidation
ln(C/C$_o$)
0.2
0.0
-0.2
-0.4
-0.6
-0.8
-1.0
-1.2
-1.4
0
2
4
6
8
10
12
14
16
Cycle

Figure S24. CV cycles of nITO|P_3 (Top Left) in fresh 0.1 M $HClO_4$ at a scan rate of 50 mV/s after soaking in 1 mM U^{4+} in 0.1 M $HClO_4$ for 10 min; and the corresponding loss of adsorbed uranium based on the reduction at -0.25 V and oxidation at 1.0 V highlighting first order loss of U(VI) and U(IV) (Top Right, and Bottom Left, Right). The initial surface coverage is 8.6 nmol/cm^2. The electrode area was 1.00 cm^2.

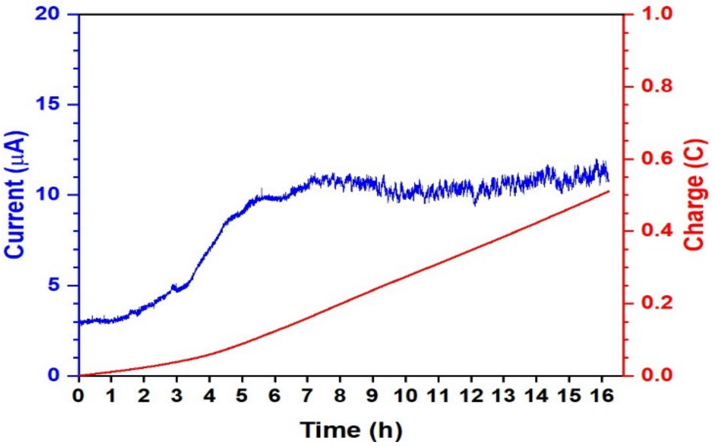

Figure S25. Bulk electrolysis at -0.20 V of 1 mM UO_2^{2+} in 0.1 M $HClO_4$ at a Pt electrode to retain some UO_2^{2+} and generate UO_2^{+} and U^{4+} in solution.

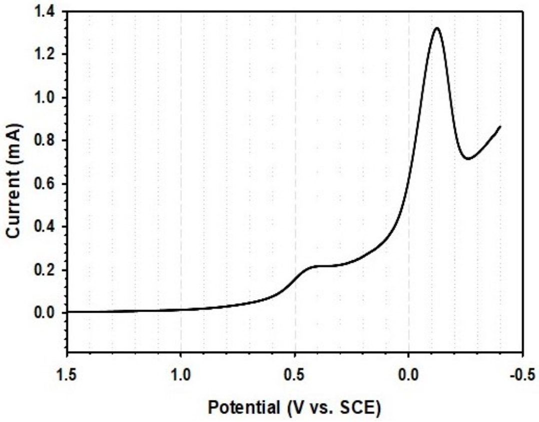

Figure S26. Square wave voltammogram at a nITO|P_3 electrode of a used 1 mM solution of UO_2^{2+} after electrolysis at -0.20 V (Figure S25) to yield UO_2^{2+} to UO_2^{+} and U^{4+} species in 0.1 $HClO_4$.

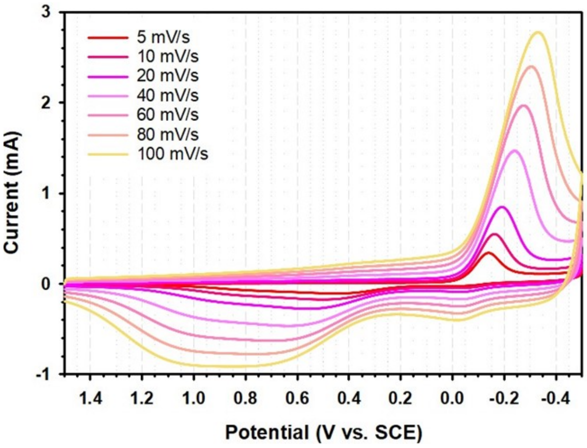

Figure S27. CVs of 1 mM UO_2^{2+} at nITO|P_3 electrode in 0.1 M $HClO_4$ + 2.9 M $NaClO_4$ at various scan rates.

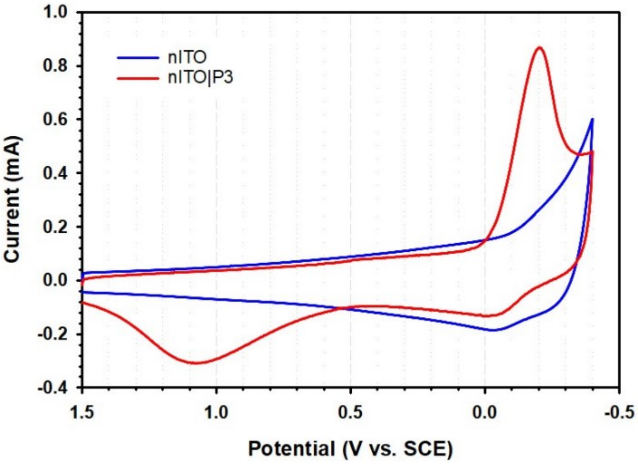

Figure S28. CV of 1 mM UO_2^{2+} at *n*ITO and *n*ITO|P_3 electrode in 3 M $HClO_4$ at a scan rate of 50 mV/s.

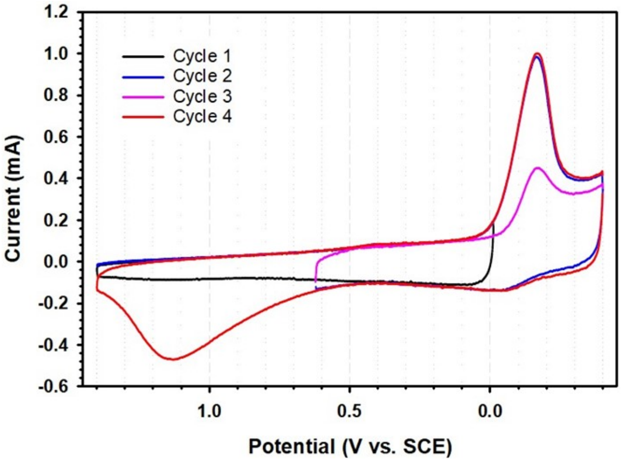

Figure S29. CVs in 3 M $HClO_4$ of a nITO|P_3 electrode soaked in 1 mM UO_2^{2+} and subsequently rinsed with 3 M $HClO_4$. at a scan rate of 50 mV/s with various scan limits. The first cycle (black) starts and ends at 0 V and scans to +1.4 V. The second cycle (blue) starts at 1.4 V and scans to -0.5 V before ending at +0.6 V (blue); the reduction of UO_2^{2+} is prominent at -0.17 V. The third cycle (pink) starts and ends at +0.6 V and scans to -0.5 V, and features a diminished UO_2^{2+} reduction. The fourth and final scan (red) is a full scan, starting at -0.5 V scanning to +1.5 V where a prominent U^{4+} oxidation is observed at +1.12 V, and then scanning back to -0.5 V where the UO_2^{2+} reduction at -0.17 V is now at the same current as the initial scan.

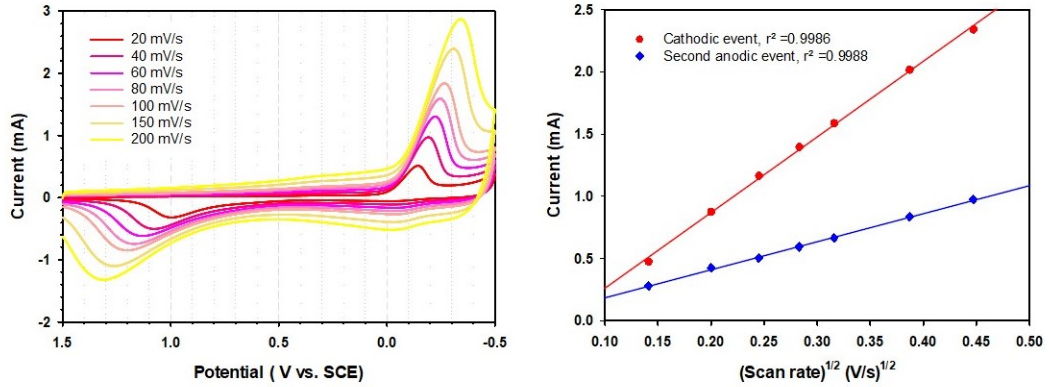

Figure S30. CVs of 1 mM UO_2^{2+} in 3 M $HClO_4$ at nITO|P_3 electrode at various scan rates. (Right) Plots of cathodic and anodic peak current versus square root of scan rate

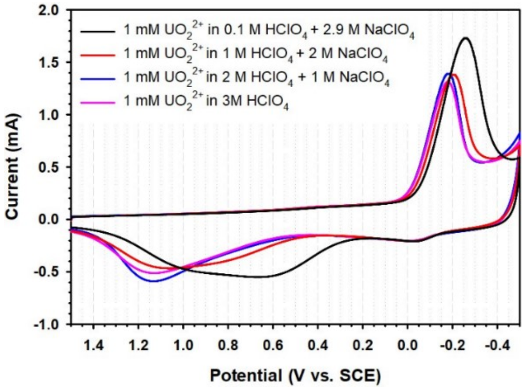

Figure S31. CVs of 1 mM UO_2^{2+} at nITO|P_3 electrode at a scan rate of 50 mV/s. $HClO_4$ concentration is varied from 0.1 M to 3 M, with added $NaClO_4$ to ensure a constant 3 M perchlorate concentration. The dependence of redox couples on proton concentration can be evaluated. UO_2 is not significant with $[H^+] > 0.1$ M. The U^{4+} oxidation and UO_2^{2+} reduction are $[H^+]$ dependent, while the UO_2^+ oxidation is not.

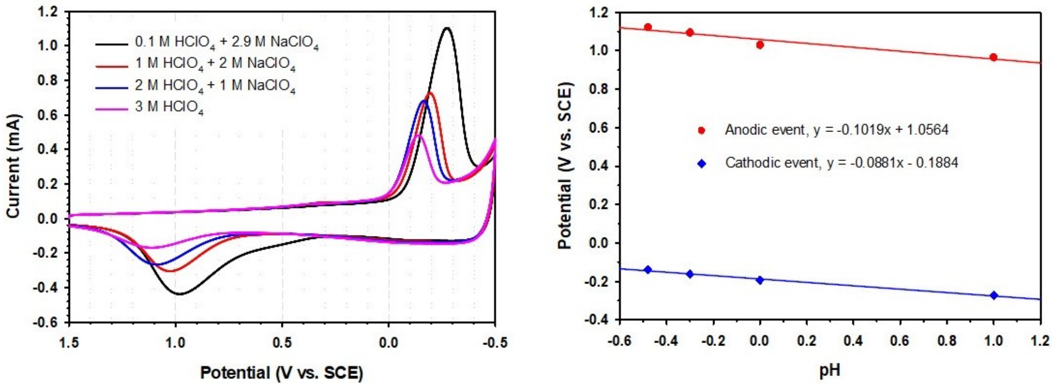

Figure S32. (Left) CVs at 50 mV/s of a nITO|P_3 electrode soaked in 1 mM UO_2^{2+} for 10 min. Perchloric acid concentration is varied from 0.1 M to 3 M, with added $NaClO_4$ to ensure a constant 3 M perchlorate concentration. The dependence of redox couples on proton concentration can be evaluated (Right), assuming that pH = -log[H^+]. UO_2 is not significant with [H^+] > 0.1 M. The U^{4+} oxidation and UO_2^{2+} reduction are [H^+] dependent, while the UO_2^+ oxidation is not.

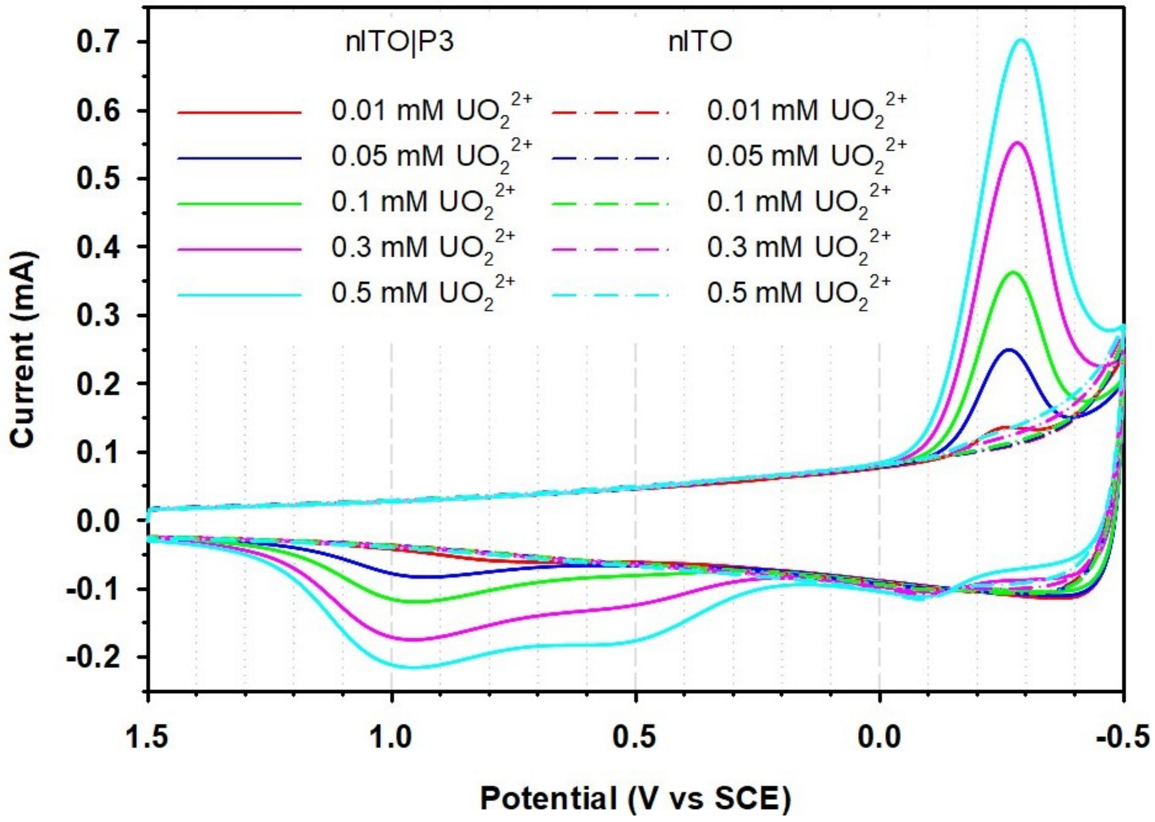

Figure S33. CVs of a nITO|P_3 electrode (solid) and bare nITO electrode (dashed line) at 50 mV/s at different concentrations of UO_2^{2+} in 0.1 M $HClO_4$. These data were used for foot-of-the-wave analysis.

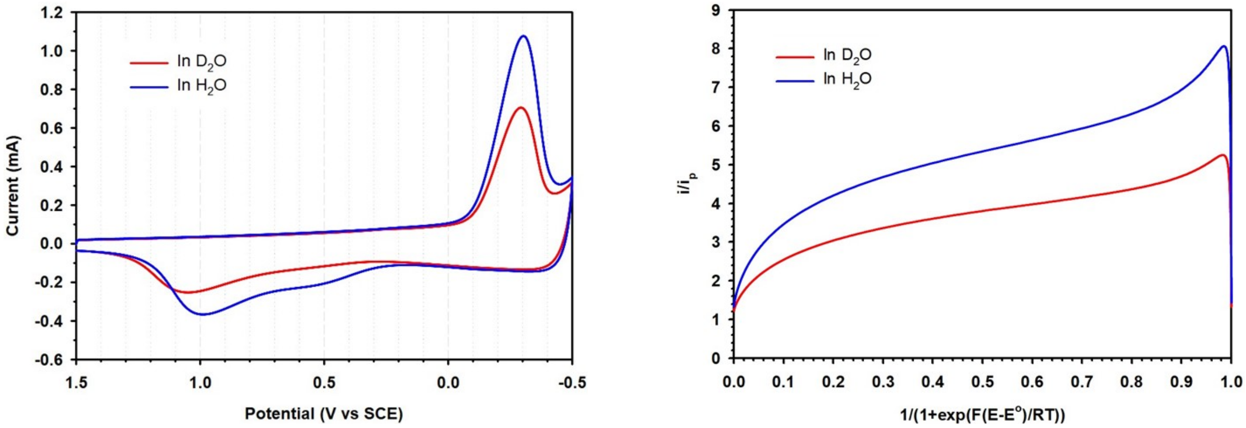

Figure S34. Left: CVs of 1 mM UO_2^{2+} at a nITO|P_3 electrode in 0.1 M $HClO_4/H_2O$ (blue), and 0.1 M $DClO_4/D_2O$ (red). These data were used for foot-of-the-wave analysis (Right) to determine the H/D kinetic-isotope ratio associated with the reduction of UO_2^{2+} to U(IV).

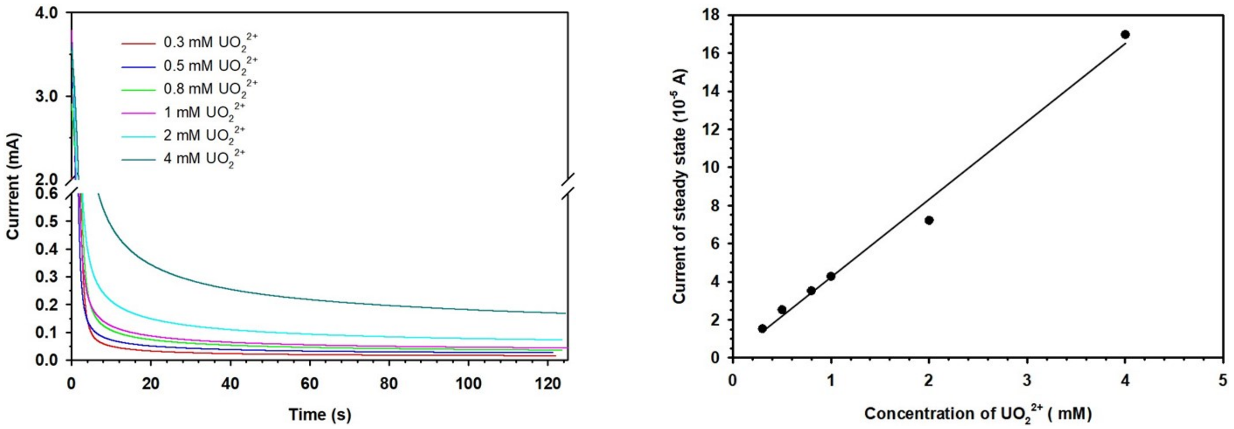

Figure S35. Left: current responses of a nITO|P_3 electrode poised at -0.4 V vs SCE in 0.1 M $HClO_4$ for 120 s at UO_2^{2+} concentrations ranging from 0.3 mM to 4.0 mM. Right: A plot of the steady-state currents in the same conditions as a function of UO_2^{2+} concentration showing a linear increase in steady state current with increasing UO_2^{2+} concentration. Using the equation $i_{cat} - i_{bg} = nFA\Gamma k_{cat}[UO_2^{2+}]$, and measuring a slope of 0.041 A/mol a second order rate constant, k_{cat} of 25 $M^{-1}s^{-1}$ is calculated.

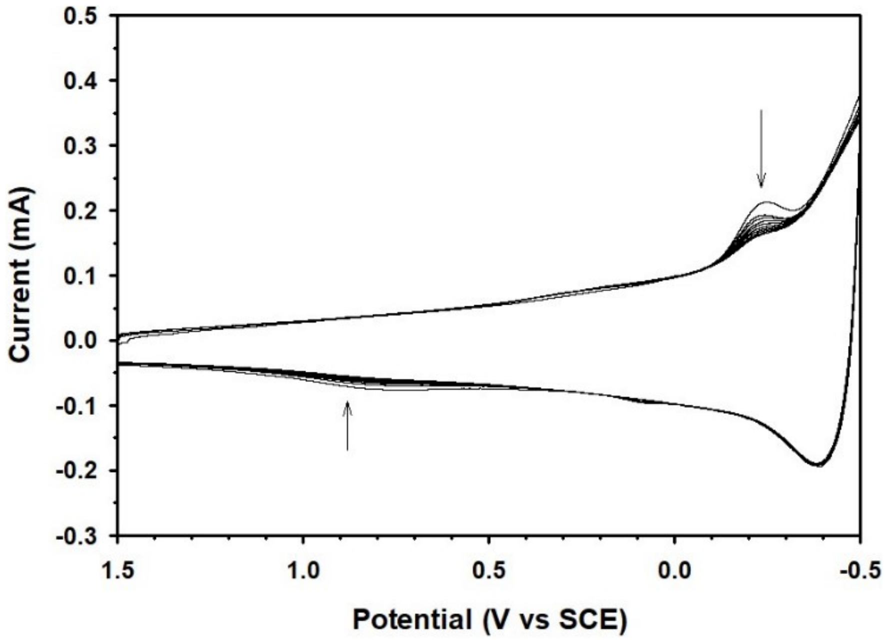

Figure S36. CVs of a monophosphate (P_1) derivatized nITO electrode (nITO|P_1) at 50 mV/s in fresh 0.1 M $HClO_4$ after soaking in 1 mM UO_2^{2+} in 0.1 M $HClO_4$ for 10 minutes.

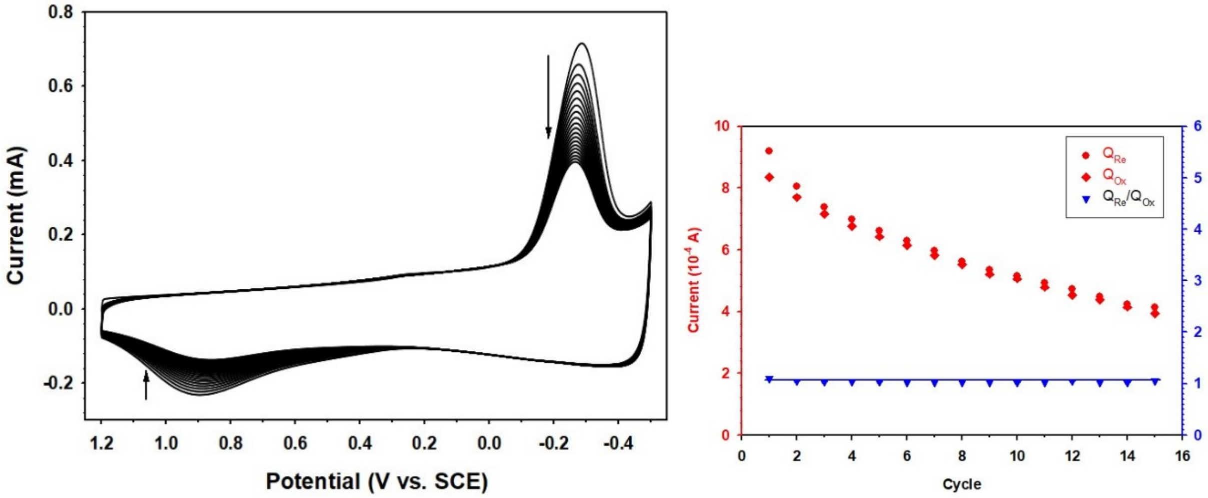

Figure S37. Left: CVs of a diphosphate (P_2) derivatized nITO electrode (nITO|P_2) at 50 mV/s in fresh 0.1 M $HClO_4$ after soaking in 1 mM UO_2^{2+} in 0.1 M $HClO_4$ for 10 minutes. Right: Plot of the ratio of charge passing through reduction events to charges passing through oxidation events at nITO|P_2 electrode in 0.1 M $HClO_4$.

Table S6. Integrated charges passing through the UO_2^{2+} reduction and U(IV) oxidation events at nITO|P_3 and nITO|P_2 electrodes in 0.1 M $HClO_4$.

Cycle number	nITO|P_3		nITO|P_2	
	Q_{Re} (10^{-4} C)	Q_{Ox} (10^{-4} C)	Q_{Re} (10^{-4} C)	Q_{Ox} (10^{-4} C)
1	9.565	8.628	9.188	8.353
2	8.839	8.055	8.047	7.699
3	8.451	7.651	7.392	7.167
4	8.102	7.332	6.995	6.764
5	7.770	7.175	6.618	6.430
6	7.555	6.950	6.294	6.146
7	7.280	6.701	5.975	5.820
8	7.065	6.463	5.632	5.524
9	6.862	6.006	5.349	5.212
10	6.629	5.926	5.146	5.066
11	6.455	5.713	4.923	4.795
12	6.207	5.548	4.733	4.529
13	6.098	5.326	4.487	4.384
14	5.926	5.290	4.223	4.148
15	5.745	5.047	4.137	3.938

Table S7. Potentials (V vs SCE) of uranium redox reactions studied under different conditions with a scan rate of 50 mV/s. ‘n.a.’ indicates that the oxidation/reduction event is not observed.

Conditions	E_{Red} (UO_2^{2+})	E_{red}(UO_2^{+})	E_{Ox} (UO_2^{+})	E_{Ox} (UO_2)	E_{Ox} (U^{4+})
nITO (0.1 M $HClO_4$)	-0.25 V	n.a.	-0.12 V	0.40 V	n.a.
nITO|P_3 (0.1 M $HClO_4$)	-0.25 V	0.25 V	-0.12 V	0.50 V	0.80 V
nITO|P_3 (0.1 M H ClO_4 + 2.9 M Na ClO_4)	-0.27 V	n.a.	-0.05 V	0.60 V	0.96 V
nITO|P_3 (1 M H ClO_4 + 2 M Na ClO_4)	-0.20 V	n.a.	-0.05 V	n.a.	1.03 V
nITO|P_3 (2 M H ClO_4 + 1 M Na ClO_4)	-0.17 V	n.a.	-0.05 V	n.a.	1.09 V
nITO|P_3 (3 M H ClO_4)	-0.14 V	n.a.	-0.05 V	n.a.	1.12 V

References

(1) Sheridan, M. V.; McLachlan, J. R.; Gonzalez-Moya, J. R.; Cortes-Medina, N. D.; Dares, C. J., Indium Tin-Doped Oxide (ITO) as a High Activity Water Oxidation Photoanode. *ACS Appl Mater Interfaces* **2021,** *13* (33), 40127-40133.

(2) Costentin, C.; Drouet, S.; Robert, M.; Savéant, J.-M., Turnover Numbers, Turnover Frequencies, and Overpotential in Molecular Catalysis of Electrochemical Reactions. Cyclic Voltammetry and Preparative-Scale Electrolysis. *J. Amer. Chem. Soc.* **2012,** *134* (27), 11235-11242.